

ANTITUMOR AND ANTIOXIDANT POTENTIAL OF *MAJORANA HORTENSIS* EXTRACT BINDING TO THE SILVER NANOPARTICLES ON LUNGS CANCER CELL LINE

Jameelah Kadhim TAHER AL-ISAWI^a,
Aeshah Muhana MOHAMMED^a, Dhafir T.A. AL-HEETIMI^{a*}

ABSTRACT *Majorana hortensis* is widely distributed in the Mediterranean area with different medicinal potentials. In the current study, 1 mmol/L AgNO₃ and 4% hydro-methanol leaf extract of *M. hortensis* at neutral pH (7.0) were successfully combined to create green *Majorana hortensis* – silver nanoparticles (MHE-AgNPs) after applying the reaction to sunlight for 30 minutes. MHE-AgNPs were characterized using atomic force microscope (AFM), high resolution-scanning electron microscope (HR-SEM) and energy-dispersive X-Ray (EDX). The size range of the MHE-AgNPs was between 50 and 95 nm, and they had a spherical form with smooth surface. With an IC₅₀ of 36.39 µg/mL, MHE-AgNPs exhibited a 2,2'-diphenylpicrylhydrazyl (DPPH) scavenging ability in a concentration-dependent manner. The MTT colorimetric technique was used to determine the MHE-AgNPs cytotoxicity against A549 cell line. The green synthesis of MHE-AgNPs markedly improved the cytotoxic action of MHE-AgNPs against A549 cells. The multiparametric cytotoxicity assay using High-content Screening was employed. MHE-AgNPs significantly reduced the cell viability, increased the membrane permeability, reduction in mitochondrial potential and stimulating the release of cytochrome c indicating the capability of MHE-AgNPs in killing A549 cells.

Keywords: *Majorana hortensis*, AgNPs, MTT Assay, Antioxidant, A549

^a Department of Chemistry, College of Education for Pure Science Ibn Al-Haitham, University of Baghdad, Baghdad / Iraq.

* Corresponding author: dhafir1973@gmail.com, dhafir.t.a@ihcoedu.uobaghdad.edu.iq



INTRODUCTION

Traditional medicinal herbs have been utilized by humans to treat illnesses for ages. Many researchers are now interested in using those medicinal plants to treat a variety of illnesses and diseases [1, 2].

The Labiatae family member *Majorana hortensis* (M.), sometimes known as sweet marjoram, is native to Mediterranean nations and was used by the ancient Egyptians, Greeks, and Romans in different applications [3]. The plant was formerly known as *Origanum majorana*. It is an aromatic plant that has culinary purposes as a result of its scent. The medicinal benefits of the plant extract include treating fevers, treating digestive issues, and acting as an expectorant. *M. hortensis* demonstrated a wide range of biological activities, including intestinal antispasmodic, stomachache, cough, rheumatism, headache, rheumatoid arthritis, allergies, fever, hypertension, respiratory infections, antidiabetic, and painful menstruation [4, 5]. Additionally, *M. hortensis* exhibits a broad range of actions, including anti-inflammatory, nephroprotective, anti-proliferative, and anti-cancer qualities. There are bioactive compounds that mediate these actions, including thymol, carvacrol, tannins, hydroquinone, sitosterol, cis-sabinene hydrate, limonene, terpinene, camphene, and flavonoids like diosmetin, quercetin, luteolin, and apigenin [6]. Two substances found in *M. hortensis*, thymol and carvacrol, have been shown to have antioxidant and antibacterial activities. Carvacrol has also demonstrated anti-proliferative properties in Hela carcinoma cells [7].

Nanotechnology is an area of study that is rapidly expanding as a result of its many uses in catalysis, solar energy, waste management, and sensing technology. Nanomaterials are successfully employed in the field of medicine for medication administration, diagnosis, cancer treatment, wound healing, auto-immune disease treatment, and the development of antibacterial agents [8, 9]. Nanomaterials' use in tissue engineering, cancer therapy, cell labeling, biological tagging, and DNA and protein detection has recently increased. Various metals such as gold [10] and silver [11] are used to create nanoparticles. They display novel physico-chemical traits that are not seen in bulk metals or individual molecules.

As a result of its many uses, silver is a popular metal employed in the creation of nanoparticles. Physical and chemical approaches for creating nanoparticles are very expensive and hazardous to the environment [12]. As a result, different techniques for biosynthesizing nanoparticles are required. This biosynthesis ought to be inexpensive, quick, simple, environmentally friendly, and non-toxic. Silver nanoparticles (AgNPs) derived from biological materials, particularly plant components, have small sizes and large surfaces [13].

AgNPs are produced by a one-step green procedure that results in stable by products. Numerous phytoconstituents found in plant materials can convert silver ions into silver nanoparticles. Plant-based nanoparticle production, shape, and topography are influenced by variables such temperature, reaction incubation time, pH, plant extract concentration, and AgNO₃ concentration [14]. The pharmaceutical industry has used silver nanoparticles that were created utilizing extracts from medicinal plants.

The objective of this research is to utilize *M. hortensis* alcoholic leaf extract to create silver nanoparticles. These nanoparticles were characterized, and their antioxidant and tumor cytotoxic activities were assessed.

RESULTS AND DISCUSSION

Biosynthesis and Characterization of MHE-AgNPs

The total yield of MHE extracted via hydro-methanol solvent was 1.81 g out of 20 g from dried leaves of *M. hortensis*. *M. hortensis* leaf extract (green) was added to an AgNO₃ solution (colorless), which was then left for 25 minutes in direct sunshine. As MHE-AgNPs were being biosynthesized, the solution's color changed from dark green to dark orange. The AFM 3D images Figure 1 A exhibited the that there were few agglomerations and that MHE-AgNPs had formed in a homogeneous distribution. The Granularity Accumulation Distribution revealed that average particle size of MHE-AgNPs was 77.01 nm. Figure 1B, shows that the produced MHE-AgNPs have a particle diameter ranges from 10 to 250 nm. This wide diameter range might be caused by the particles sedimentation which would reduce their absorption [15, 16].

According to the results of the High-Resolution Scanning Electron Microscope (HRSEM), the synthesized MHE-AgNPs were spherical in form and ranged in size from 50 to 95 nm Figure 2 with mean particle size of 80.05±19.08. Some nanoparticles were larger than others, which may be the result of particle aggregation or overlapping. By using HRSEM imaging, the size, shape, and morphology of the produced green nanoparticles were confirmed. Numerous researchers have regularly employed HRSEM to characterize nanoparticles [17]. The MHE-AgNPs HRSEM image demonstrated that these particles contained a smooth surface, were spherical in shape, and highly stabilized.

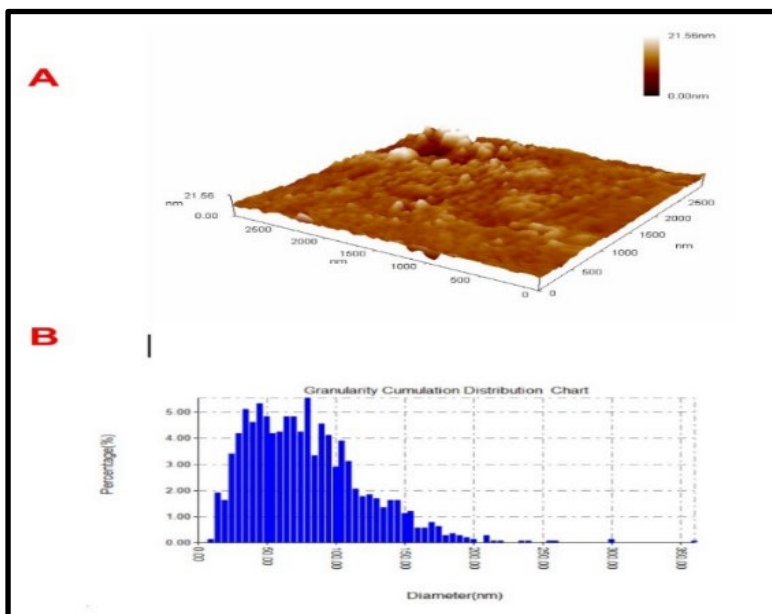


Figure 1. (A) AFM image of MHE-AgNPs. (B) The corresponding Granularity Accumulation Distribution with average particle size.

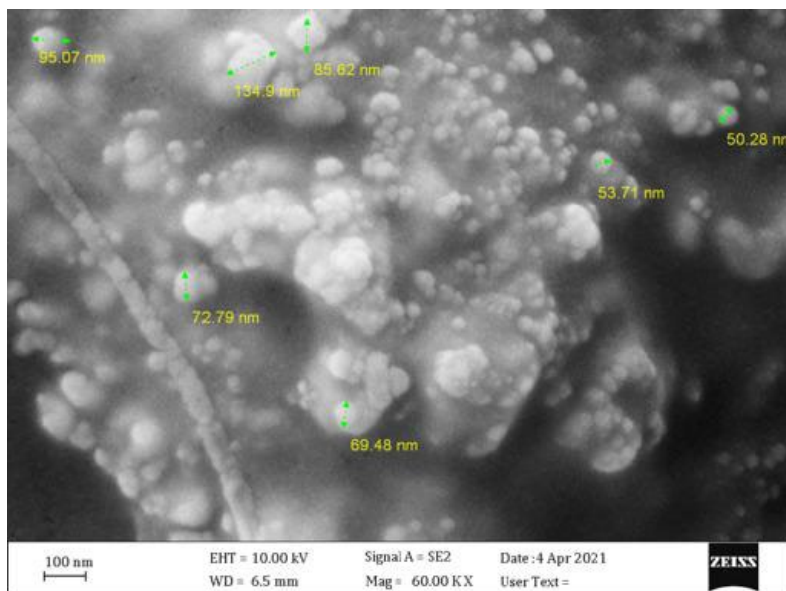


Figure 2. HRSEM micrograph of AgNPs synthesized using leaf extract of *M. hortensis*.

The EDS spectra of AgNPs were recorded at 3 keV, which clearly showed a strong spectral signal in the silver region Figure 3. The formation of MHE-AgNPs strongly supports for the spectra of AgNPs. The presence of oxygen and carbon signals in the EDS spectra suggests the presence of biomolecules (proteins and carbohydrates) adjacent to MHE-AgNPs.

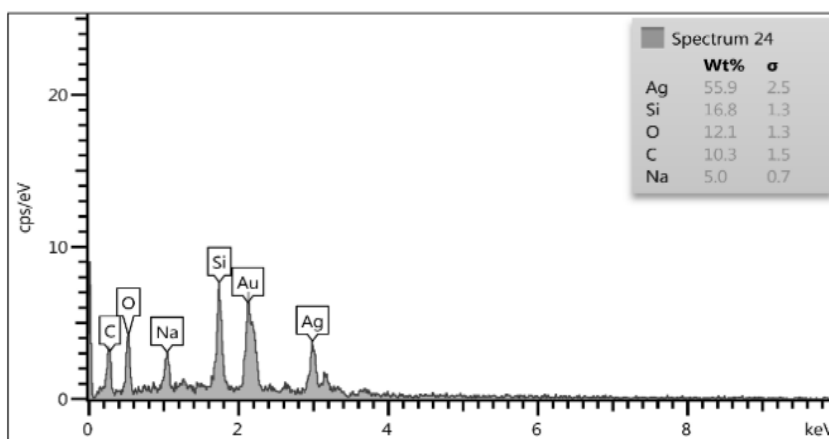


Figure 3. Energy-Dispersive X-Ray spectrum of MHE-AgNPs.

The Scavenging Activity of MHE-AgNPs

By utilizing ascorbic acid as a positive reference, the DPPH scavenging test was used to measure the antioxidant activity of MHE and MHE-AgNPs. The degree of DPPH scavenging capability was directly correlated to MHE and MHE-AgNPs applied concentrations. The value of calculated IC_{50} for MHE and MHE-AgNPs were 105.3 and 36.39 $\mu\text{g/mL}$, respectively, while the IC_{50} of ascorbic acid treatment was 27.47 $\mu\text{g/mL}$. These findings demonstrated that MHE-AgNPs improved MHE in terms of free-radical scavenging capacity. MHE and MHE-AgNPs both had an increase in scavenging power in concentration-dependent pattern. Compared to MHE, MHE-AgNPs had a much higher scavenging activity Figure 4. Numerous researchers have earlier reported similar findings of increased DPPH scavenging activity by using metallic NPs like gold, platinum, and silver NPs [18, 19]. The enhanced scavenging activity of *M. hortensis* leaves extract coupled with AgNPs might be connected to phenolic compounds, which were crucial in stabilizing lipid peroxidation. Previous research demonstrated that *M. hortensis* essential oils, ethanolic extract, water, methanol, and chloroform extracts all exhibited strong antioxidant activity [20].

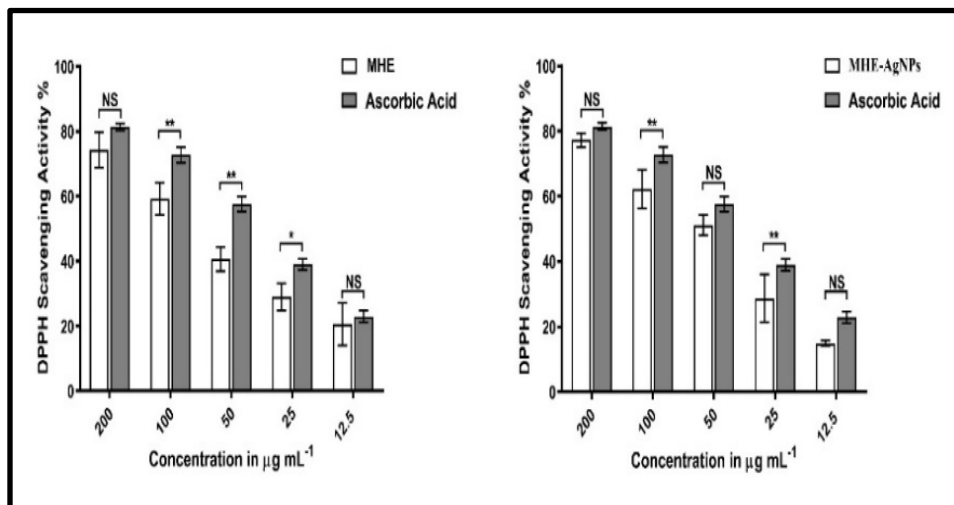


Figure 4. DPPH scavenging activity of MHE (left) and MHE-AgNPs (right). Data expressed as mean \pm SD percentage antioxidant activity compared with ascorbic acid. *: $p < 0.05$, **: $p < 0.01$, NS: Non-significant.

Cytotoxic Activity of MHE-AgNPs Against A549 Tumor Cell Line

With over 1 million deaths in 2020, lung cancer remained the most common cause of cancer death worldwide, accounting for nearly 18% of all cancer deaths [21]. To ascertain the impact of MHE and MHE-AgNPs on the *in vitro* viability of A549 cells, the MTT test was used in the current investigation. The untreated cells, which had 100% cell viability, were considered as the control cells. Better cell viscosity was observed in the MHE and MHE-AgNPs-treated cells at concentrations of 12.5 and 50 $\mu\text{g/mL}$, indicating that at low concentrations, MHE and MHE-AgNPs treatments were not significantly different from control treatments in terms of cytotoxicity. The viability of cells was considerably ($p < 0.05$) decreased at higher concentrations of MHE-AgNPs (50–400 $\mu\text{g/mL}$) compared to MHE alone (Table 1).

The IC_{50} of MHE and MHE-AgNPs treatments were 51.38 and 17.75 $\mu\text{g/mL}$, respectively, indicating the significant improvement in inhibiting A549 cells by coupling MHE with AgNPs. These findings revealed that the MHE-AgNPs significantly decreased the metabolic activity of cancer cells.

Many studies that have demonstrated the dose-dependent reduction of growth of human cancer cell lines, such as fibrosarcoma, leukemia and lung cancer cells [22]. According to an Indian study, the potent anti-tumor

biological effects of *M. hortensis* on cancer cells attributed to the plant's high concentration of polyphenols, flavonoids, and tannins in its chemical makeup. P-coumaric acid has shown that it can stop the proliferation of tumor cells by inducing mitochondrial malfunction and cell death [23]. The antiproliferative impact of MHE was significantly enhanced by the addition of AgNPs. AgNPs made from Piper longum fruit extract have an IC₅₀ of 67 µg/mL against the Hep-2 cell line, making them cytotoxic [24]. Likewise, AgNPs produced from *Origanum vulgare* showed LD₅₀ of 100 µg/mL against A549 cells [25]. In fact, reactive oxygen species, which damage cellular components like DNA, proteins, and lipids and ultimately result in the death of cancer cells, may be induced by AgNPs [26].

Table 1. Mean (±SD) cytotoxic effect (%) of MHE and MHE-AgNPs against A549 cell line for each concentration used in this study at 37°C for 24 hrs. (*n* = 3).

A549			
Concen. µg mL⁻¹	Inhibition % (Mean±SD)		<i>p</i> value
	MHE	MHE-AgNPs	
400	50.81±0.69	67.45±4.43	< 0.0001 **
200	46.84±2.61	64.59±3.83	< 0.0001 **
100	39.2±2.1	54.95±3.59	0.0002 **
50	24.48±4.61	36.96±3.52	0.0029 **
25	13.02±5.96	19.68±6.36	0.2261 NS
12.5	4.05±1.03	3.63±1.17	0.9998 NS

***p* < 0.01, NS: Non-significant.

Multiparametric Toxicity of MHE-AgNPs

MHE-AgNPs were used to carry out a multi-parameter cytotoxic activity via High Content Screening (HCS) against A549 cells. In this assay, five different metrics (cell count vitality, nuclear intensity, cell membrane permeability, mitochondrial membrane potential, and cytochrome C release) were identified.

As MHE-AgNPs doses increased, the viable count of A549 cells decreased in comparison to untreated cells, according to the results shown in Figure 5. Only treatments with MHE-AgNPs at concentrations of 100 and 200 µg/mL showed a significant (*p* 0.0001) reduction in cell viability at rates of 34.3 and 38.1%, respectively. According to the MTT experiment, in which the drop in cell number was dose-dependent, this finding strongly implies that MHE-AgNPs are cytotoxic to A549 cells.

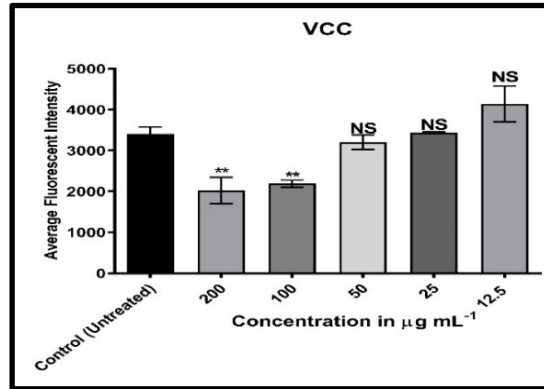


Figure 5. Mean (\pm SD) fluorescent intensity of A549 cell count after treatment with MHE-AgNPs (12.5, 25, 50, 100 and 200 $\mu\text{g/mL}$) compared with untreated cells for 24 hrs. NS: Non-significant, **: $p \leq 0.01$. SD: Standard Deviation, ($n = 3$).

In Figure 6A, 100 and 200 $\mu\text{g/mL}$ MHE-AgNPs treatments significantly ($p = 0.0001$) raised the nuclear intensity of A549 cells by 1.3 and 1.7-fold in comparison to untreated cells, respectively. Apoptotic indicators are directly correlated with nuclear intensity changes such as chromatin condensation, cellular DNA fragmentation, cell shrinkage, and blebbing [27]. The intensity of the cell membrane permeability, on the other hand, was significantly ($p = 0.0022$) altered in A549 cells treated with 200 $\mu\text{g/mL}$ MHE-AgNPs as compared to untreated cells, as shown in Figure 6B.

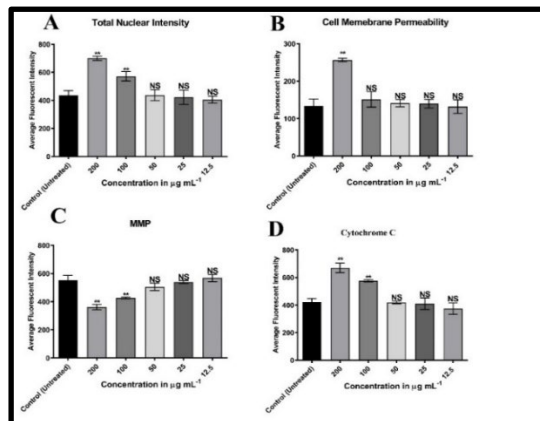


Figure 6. Mean (\pm SD) fluorescent intensity of A549 cell nuclei (A), membrane permeability (B), mitochondrial membrane potential (C) and cytochrome C release (D), after treatment with MHE-AgNPs (12.5, 25, 50, 100 and 200 $\mu\text{g/mL}$) compared with untreated cells for 24 hrs. NS: Non-significant, **: $p \leq 0.01$. SD: Standard Deviation, ($n = 3$).

Results Increases in MHE-AgNPs concentration resulted in a dose-dependent reduction in MMP intensity, with a significant ($p < 0.0001$) reduction of 26% at 200 $\mu\text{g/mL}$, as shown in Figure 6C. The translocation and release of cytochrome c from mitochondria into the cytoplasm were significantly ($p < 0.0001$) caused by the collapse of mitochondria in A549 cells treated with MHE-AgNPs at doses of 100 and 200 $\mu\text{g/mL}$.

The high-content screening test is regarded as a predictive assay for monitoring morphological alterations of cells caused by toxic effects since it enables quantitative measurements of numerous toxicity-related parameters [27, 28]. The number of A549 cells significantly decreased as MHE- AgNPs concentration increased, which may have been a direct result of cell death being triggered. The loss of plasma membrane integrity is strongly related to a toxic or apoptotic effect [29]. Since membrane permeability dye can only penetrate and stain cells with damaged membranes, the increased intensity of the dye strongly supports the idea that MHE-AgNPs at greater concentrations clearly produced cell membrane damages and hence prompted apoptosis. Such observations are often linked to a variety of cell death mechanisms, such as specific rearranging processes that cause the plasma membrane to lose integrity [30].

Results showed that at 100 and 200 $\mu\text{g/mL}$ of MHE-AgNPs significantly reduced mitochondrial brightness when compared untreated cells. The induction of apoptosis in A549 cells may be due to alterations in the mitochondrial transmembrane potential. Finally, cysteine proteases, which are primarily in charge of breaking down and digesting cells from the inside, are activated by the release of cytochrome c which eventually introduce the cells into apoptosis [31].

CONCLUSIONS

We can conclude that under sunlight exposure, a hydro-methanol leaf extract of the medicinally significant *M. hortensis* plant was successfully employed to synthesize stable AgNPs. MHE-AgNPs biogenesis was verified using AFM, HRSEM and EDX. MHE-AgNPs were formed in a spherical shape with homogenous distribution, few aggregations and within nanoscale range. MHE-AgNPs significantly showed a great antioxidant activity and cytotoxic action against a lung carcinoma cell line (A549) compared with MHE. The results of HCS highly proved the cytotoxic activity of MHE-AgNPs in dose-dependent pattern suggesting that bio-formation of MHE-AgNPs ameliorate the potential cytotoxicity of MHE.

EXPERIMENTAL (METHODS)

Plant Material and *M. hortensis* Extract (MHE) Preparation

M. hortensis leaves were obtained from a local garden nursery in Baghdad, Iraq, between February and April of 2022. The plant was recognized by a botanist from Al-Mustansiriyah University/College of Science. The cut plant was left to dry for two weeks in the shade at room temperature. 20 g of the plant material was extracted for 4 hours at 40°C in 200 mL of hydro-methanol (80:20). The extracted materials were then separated using Whatman's No. 1 filter paper. A rotary vacuum evaporator was used to evaporate the remaining solvent. The following equation was used for determining the yield of the extracted material: $\text{yield (\%)} = (\text{The weight of the extracted material} / \text{The weight of the original plant material}) \times 100$.

Biosynthesis of Ag NPs Using *M. hortensis* Extract

A 100 mL solution of 1 mmol/L aqueous silver nitrate (AgNO_3) was mixed with 4% MHE to create nanoparticles. The reaction mixture's pH was adjusted to 7.0. The reaction mixture was held in a flask that was kept at 38°C and intense solar light (65000 lux). Under direct sunlight, various variables including sunlight exposure period (0–30 min), AgNO_3 concentration (0.5–5 mmol/L), and MHE inoculum dose (0.5–6.0%) were assessed one at a time to maximize the biosynthesis of MHE-AgNPs. The water-soluble biological residues were removed from the MHE-AgNPs synthesized using centrifugation at 15,000 rpm for 30 min before being re-dispersed in deionized water. Washing step was repeated several times and the pellet containing MHE-AgNPs was air-dried at room temperature.

Characterization of MHE-AgNPs

Atomic Force Microscope

Using the NTEGRA (NT-MDT) equipment (Spectrum Instrument, Limerick, Ireland), the surface morphology and average particle size of the nanoparticles were examined. Before analysis, samples were prepared by casting drops of MHE-AgNPs solution onto glass slides and allowed to air dry at room temperature.

High Resolution Scanning Electron Microscope (HRSEM)

The morphology and size of MHE-AgNPs were examined using HRSEM (ZEISS Gemini 300, Germany). Drops of MHE-AgNPs solution were cast onto glass slides to create the SEM samples, which were then allowed to air dry at ambient temperature. SEM pictures was captured at scale of 100 nm. Using ImageJ software, SEM pictures were processed to determine the mean diameter of length and area (30 measurements).

High Resolution-Scanning Electron Microscope-Energy-Dispersive X-Ray

The elemental composition, purity and morphology of the sample were examined using HRSEM and energy-dispersive X-ray (EDX). A drop of ultrasonically colloiddally re-dispersed MHE-AgNPs was dried over thin aluminum foil for two hours before being coated with gold for HRSEM-EDX analysis.

DPPH Scavenging Activity

As previously described [32], the DPPH radical scavenging assay for MHE and MHE-AgNPs was conducted. The reference utilized was ascorbic acid. In methanol, DPPH solution (0.004%) was prepared. Different concentrations of samples (12.5-200 $\mu\text{g/mL}$) were prepared in methanol and DPPH solution (2.96 mL) was added. For 20 minutes, the reaction mixture was incubated at ambient temperature and in complete darkness. After 20 minutes, the reaction mixture's absorbance was measured at 517 nm using a UV-Vis spectrophotometer (CE1021, Cecil, Italy). DPPH served as control. The percentage of scavenging activity was calculated using the following equation:

$$\text{Inhibition(\%)} = \frac{\text{Absorbance of the } - V_{e\text{control}} - \text{Absorbance of the sample}}{\text{Absorbance of the } - V_{e\text{control}}} \times 100$$

Cell Lines and Cell Line Maintenance

A human lung adenocarcinoma cell line A549 (ATCC, CCL-185) and normal WRL68 (ATCC, CL-48) cell line were supplied from Al-Nahrain Biotechnology Center/Al-Naharin University. concentration. Cells were grown in RPMI-1640 media contained 10% fetal bovine serum, 10^3 IU of penicillin G, and 0.001 g of streptomycin per 100 mL of media. A humidified incubator with 5% CO_2 was used to incubate the cells at 37°C . A549 cells were seeded at a density of 2×10^4 cells mL^{-1} into tissue culture flasks. Cells were detached

after a quick trypsinization (50 mg mL⁻¹) when they entered the exponential growth phase (between 36 and 48 hours), and then they were seeded at the desired concentration. All reagents and media were purchased from Merck (Germany).

Cytotoxicity Test (MTT Assay)

Using the MTT colorimetric assay, the cytotoxic potential of MHE and MHE-AgNPs was evaluated against A549 and WRL-68 cells. 96 flat bottom plates were seeded with an aliquot of 200 μ L of suspended cells (1 x 10⁵ cells mL⁻¹) in culture media, and the plates were then incubated for 24 hours at 37°C with 5% CO₂. A variety of concentration for each treatment (12.5 – 400 μ g mL⁻¹) were introduced to the wells after the medium had been removed from the incubation period. Cells without any treatment used as control (cells treated with serum-free media).

For an additional 24 hours, plates were incubated at 37°C and 5% CO₂. 10 μ L of MTT solution was then added to each well, and the plates were then incubated at 37°C with 5% CO₂ for another 4 hours. After properly decanting the media, 100 μ L of the solubilization solution (DMSO) was added after waiting five minutes. Using an ELISA reader (Bio-Rad, USA), the final response (formazan formation) was revealed at 575 nm. The experiment was performed in triplicate. The cytotoxicity was expressed as IC₅₀ and the formula used to calculate viability (%) was as follows:

$$\text{Viability (\%)} = \text{OD control} - \text{OD sample} / \text{OD Control} \times 100$$

Multiparametric Cytotoxic Activity of MHE-AgNPs

After being exposed to MHE-AgNPs *in vitro*, the five orthogonal A549 cell health parameters were measured using the Cellomics multi-parameter HCS cytotoxicity 3 kit (Cat. No.2069). The variables were the number of viable cells, total nuclear intensity, permeability of the cell membrane, permeability of the mitochondrial membrane, and cytochrome *c* release. In brief, A549 cells were treated for 24 hours with various doses of MHE-AgNPs (12.5 – 200 μ g/mL), and then cells were stained for 30 minutes at 37°C with cell staining solution (MMP dye + permeability dye). A549 cells were subjected to fixation, permeabilization and blocking prior to probing with primary cytochrome *c* antibody and secondary Daylight 649 goat anti-mouse IgG conjugate for 60 minutes each. Utilizing the Cellomics Array Scan HCS analyzer, plates were examined (ThermoScientific, USA).

Statistical Analysis

Graph Pad Prism version 9.0 (Graph Pad Software Inc., La Jolla, CA) was used for all statistical analyses. To determine the differences between the several groups, a one-way and two-way analysis of variance (ANOVA) (Tukey's post hoc test) were used. The statistical thresholds for significance were * p 0.05 or ** p 0.01 for all data given as mean standard deviation. Triplicates of each experiment were run independently ($n = 3$).

REFERENCES

1. N.D. Jaafar; A.Z. Al-Saffar; E.A. Yousif, *Int J Toxicol*, **2020**,39(5), 422-432.
2. R.M. Al-ezzy; R.S. Alanee; H.M. Khalaf , *Iraqi J. Sci.*, **2022**, 63(9),3703–3710.
3. F. Bina; R. Rahimi, *eCAM*, **2017**, 22(1),175-185.
4. E.N. Fatima-Zahra; R.F. Fouzia; R.A. Abdelilah; *Asian J. Pharm. Clin. Res.*, **2017**, 10, 121-130.
5. H. Hajlaoui; H. Mighri; M. Aouni; N. Gharsallah; A. Kadri; *Microb. Pathog.*, **2016**, 95, 86-94.
6. H. Makrane; M. El Messaoudi; A. Melhaoui; M. El Mzibri; L. Benbacerand; M. Aziz, *Adv Pharmacol Sci*, **2018**, 2018, 3297193.
7. M.R. Abd EL-Moneim; S.H. Esawy; E.M. El-Hadidy; M.A. Abdel-Salam, *Adv. food sci.*, **2014**,36(2), 58-64.
8. A.M. Al-Rahim; R. AlChalabi; A.Z. Al-Saffar; G.M. Sulaiman; S. Albukhaty;T. Belali; E.M. Ahmed; K.A. Khalil, *Anim. Biotechnol.*, **2021**, 1-17.
9. A.G. Oraibi; H.N. Yahia; K.H. Alobaidi, *Scientifica*, **2022**, 2022, 1-10.
10. R.I. Mahmood; A.K. Abbass; N. Razali, A.Z. Al-Saffar; J.R. Al-Obaidi, *Int J Biol Macromol*, **2021**, 184,636-647.
11. Z.A.; Ratan, M.F. Haidere; M.D. Nurunnabi; S.M. Shahriar; A.S. Ahammad; Y.Y. Shim; M.J. Reaney; J.Y. Cho, *Cancers (Basel)*, **2020**, 12(4), 855.
12. S. Ahmed; M. Ahmad; B.L. Swami; S., Ikram, *J. Adv. Res.*, **2016**,7(1), 17-28.
13. J. Mittal; A. Batra; A. Singh; M.M. Sharma, *ANSN*, **2014**,5(4),1-11.
14. Caro, C., Castillo, P.M., Klippstein, R., Pozo, D. and Zaderenko, A.P. Silver nanoparticles: sensing and imaging applications, in *Silver nanoparticles*, D.P. Perez; InTech, Croatia, chapter 11, **2010** ,201-224.
15. A.A. Moosa; A.M. Ridha; M.H. Allawi, *IJCET*, **2015**, 5(5) , 3233-3241.
16. M. Delay; T. Dolt; A. Woellhaf, R. Sembritzki; F.H. Frimmel, *J. Chromatogr. A*, **2011**, 1218(27), 4206-4212.
17. M. Baláž; N. Daneu; Ľ. Balážová; E. Dutková; Ľ. Tkáčiková; J. Briančin; M. Vargová; M. Balážová; A. Zorkovská; P. Baláž, *Adv. Powder Technol.*, **2017**, 28(12), 3307-3312.
18. A. Watanabe; M. Kajita; J. Kim; A. Kanayama; K. Takahashi; T. Mashino; Y. Miyamoto, *Nanotechnology*, **2009**, 20(45), 1-10.

19. K.H. Oh; V. Soshnikova; J. Markus; Y.J. Kim; S.C. Lee; P. Singh; V. Castro-Aceituno; S. Ahn; D.H. Kim; Y.J. Shim; Y.J. Kim, *Artif.Cells Nanomed Biotechnol.*, **2018**, *46*(3), 599-606.
20. G. Semiz; A. Semiz; N . Mercan-Doğan, *Int. J. Food Prop.*, **2018**, *21*(1),194-204.
21. X. Chen; S. Mo; B. Yi, *BMC Public Health*, **2022**, *22*(1),1-13.
22. A.A. Refaie; A. Ramadan; A.T. Mossa, *Asian Pac. J. Trop. Med.*, **2014**, *7*, S506-S513.
23. S.K. Jaganathan; E. Supriyanto; M. Mandal, *WJG*, **2013**, *19*(43),7726-7734.
24. N.J. Reddy; D.N. Vali; M. Rani; S.S. Rani, *Mater. Sci. Eng. C*, **2014**, *34*, 115-122.
25. R. Sankar; A. Karthik; A. Prabu, S. Karthik; K.S. Shivashangari; V. Ravikumar, *Colloids Surf. B*. **2013**, *108*, 80-84.
26. T. Xia; M. Kovochich; J. Brant; M. Hotze; J. Sempf; T. Oberley; C. Sioutas; J.I. Yeh; M.R. Wiesner; Nel, A.E., *Nano Lett.* ,**2006** ,*6*(8) ,1794-1807.
27. L.Jamalzadeh; H. Ghafoori ;M. Aghamaali; R. Sariri, *Iran J Biotechnol*, **2017**, *15*(3), 157-165.
28. A.G. Al-Dulimi; A.Z. Al-Saffar; G.M. Sulaiman; K.A. Khalil; K.S. Khashan; H.S. Al-Shmgani; E.M Ahmed, *J. Mater. Res. Technol.*, **2020**,*9*(6),15394-15411.
29. C. Dias; J. Nylandsted, *Cell Discov.*, **2021** ,*7*(1), 1-18.
30. N.A. Hadi; R.I. Mahmood; A.Z. Al-Saffar, *Gene Rep.*,**2021** , *24*, 101285.
31. S. Verma; R. Dixit; K.C. Pandey, *Front. Pharmacol.*, **2016**,*7*, 1-12.
32. A.Z. Al-Saffar; N. A. Hadi; H. M. Khalaf, *Indian J. Forensic Med. Toxicol.*, **2020**, *14*(3) ,2492-2499.